Model for the generation of leptonic mass. II

David Fryberger

Stanford Linear Accelerator Center, Stanford University, Stanford, California 94305

(Received 6 April 1981)

An analysis of a model for the generation of leptonic mass that considered only symmetric solutions is extended to include the possibility of asymmetric solutions. This possibility arises from a breakdown of a permutation symmetry between muon and electron. This broken symmetry also furnishes in a natural way a quantum number which distinguishes muons from electrons. A numerical study of the solutions of the extended model is performed, and it is shown that indeed their structure has a region with asymmetric solutions. The observed μ-e mass ratio lies within the range of estimates using this model, but the mass-splitting estimates thus obtained are seen to be very sensitive to computational errors as well as assumptions about unknown non-QED physics. The reasons for this sensitivity and sources of these errors are discussed. By an extrapolation of the model beyond the τ, a new yet heavier lepton is predicted, and a comparison is made to those predicted by some other models. Experimental tests of these predictions shoud be possible using coming generations of accelerators.

I. INTRODUCTION

Recently a self-consistent model for the generation of leptonic mass was proposed,[1] hereafter referred to as I. In I, symmetric solutions (equal masses) were studied. Since the work herein is an extension of I to investigate the possibility of asymmetric solutions (unequal masses) a brief review of I is in order.

The basis of I is the fact pointed out by Heisenberg and co-workers[2] that since the equations of quantum field theory are nonlinear, symmetries present in those equations may not be manifest in their solutions. Developing this idea along different lines, it has been proposed[3] that a dynamical symmetry breaking could lead to self-consistent solutions with nonzero fermion mass. A fermion model with dynamically generated physical masses was considered by Baker and Johnson,[4] who found that consistency required a null bare mass. While this scheme breaks the formal γ_5 invariance that obtains in QED having fermions described by the massless Dirac equation, it has been shown[5] that the breaking of this γ_5 symmetry is immune to the Goldstone-boson dilemma.[6]

In the formulation in I, then, it was assumed that the bare lepton masses are zero, the physical masses being totally dynamic, deriving from the QED self-interaction. This assumption leads to the self-consistency equation

$$\frac{\delta m_i}{m_i} = 1 , \qquad (1)$$

which is to be satisfied by the (approximations to) δm_i, the QED self-masses. Equation (1), of course, applies only to the charged leptons. It is worth mentioning that since leptonic mass in this model is due to the self-interactions of electric

charge, the observed fact that neutrinos are massless, or nearly so, finds a natural explanation: they are electrically neutral.

Figure 1 shows a graphic depiction of the general functional expression[7] for fermion self-mass. In terms of renormalized quantities, a self-consistent perturbation expansion for the QED self-mass was developed, and it was shown that a sum of graphs containing vacuum polarization loops diverges *before* the momenta reach infinity. This causes a singularity in the (completely renormalized) photon propagator (which point we use to define the "Landau mass" M_L) first found by Landau and his co-workers,[8] who used a somewhat different analysis. This difficulty, i.e., a non-Borel summable set of graphs,[9] has also been shown to exist in the perturbation expansion for the anomalous magnetic moment.[10]

Within the above framework, there appears to be no obvious means to eliminate this singularity in the complete photon propagator[11]; renormalization circumvents the difficulty without addressing
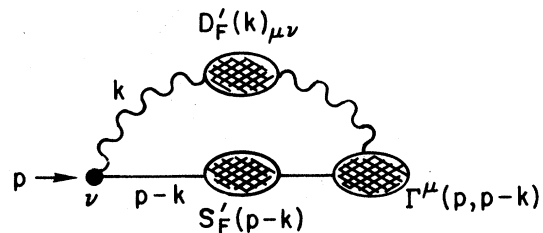

FIG. 1. A graphical depiction of $\Sigma(p)$, the proper self-energy of a fermion of four-momentum p. $D'_F(k)_{\mu\nu}$ is the complete photon propagator, $S'_F(p-k)$ is the complete fermion propagator, and $\Gamma^\mu(p, p-k)$ represents the vertex function. The cross hatching indicates that these QED functions are complete summations of the appropriate proper Feynman (sub) graphs.

it. (Of course, the grand unification schemes offer another possible resolution of this difficulty. The motivation for not pursuing this avenue was discussed in I.) Accordingly, the Landau singularity is a feature of the model in I as well as in its extension here. It is tacitly accepted that this singularity is a mathematical abstraction of physical aspects of pointlike fermions.

It was shown in I that self-consistent solutions for a dynamically generated leptonic mass could be obtained by utilizing an abrupt or "hard" ultraviolet cutoff put in by hand just below the Landau singularity. In order to eliminate this arbitrary cutoff and still obtain convergent expressions, it was assumed that the functional form of the complete photon propagator is the same above the Landau singularity as it is below and that there is a physical cutoff at the Landau singularity. The use of this (phenomenological) cutoff implies that there is structure to the electronic charge with a scale of the Landau length $(\hbar/M_L c)$. Landau and his collaborators[8] long ago considered such structure as a possibility; unfortunately, structure on this scale ($\sim 10^{-33}$ cm) is well below present experimental observability[12] and hence resides in the realm of theoretical speculation. Nevertheless, this concept has received considerable attention, in particular in connection with the gravitational interaction.[13]

In this formulation, then, the momentum integrations in the expressions for the self-mass are extended to infinity. Using analytic continuation to extend the domain of the expression for the photon propagator assumes that the functional form found by summation of the perturbation series, which is (presumed to be) valid below the Landau singularity (or Landau mass) is of greater significance as a solution to the problem than the original series itself. This philosophy is in the same vein as that employed in Borel's method of summation.[14] Thus, while the perturbation expansion is clearly not a complete solution to the self-mass problem, it furnished the mathematical basis for this model which offers a possibility of solution.

Following these ideas, the perturbation expansion for leptonic self-mass was converted to a series in which the order n_γ denotes the number of photons, each photon carrying (an approximation to) its own vacuum polarization. In the limit wherein $n_\gamma = \infty$, the graphs of this expansion can be put into a one-to-one correspondence with the graphs of the usual expansion in which the order or power of the electron charge $n_e = \infty$. In this new series, however, the Landau singularity is contained in the (dressed) photon propagator, but with the above assumptions its divergence is now
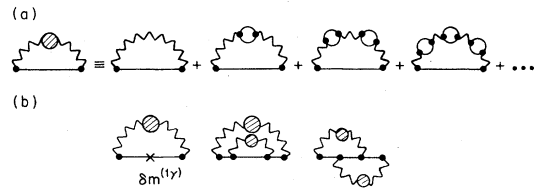
FIG. 2. (a) The one-photon fermion self-mass graph (left-hand graph with the hatching) is defined as the sum of graphs of vacuum polarization loops indicated on the right-hand side of the equation. From this series approximation is derived the one-photon estimate of the self-mass $\delta m^{(1\gamma)}$. (b) The additional graphs which are used to define $\delta m^{(2\gamma)}$, the two-photon piece of the fermion self-mass. The hatching indicates vacuum polarization loop sums as in (a).

under control. Thus, this formulation for the self-mass is well defined since there is an effective, self-consistent ultraviolet cutoff and the non-Borel summability problem (or Landau singularity) is not evident in the other divergent quantities of QED, i.e., the fermion propagator and the vertex function.

Using a leading-logarithm approximation, good agreement with the Landau result was obtained with one photon, dressed as in Fig. 2(a). A two-photon self-mass calculation was also carried out in I [see Fig. 2(b)], giving results which were qualitatively the same as, and quantitatively close to, the one-photon calculation. It is conjectured that higher-order expansions with additional photons would exhibit no further qualitative changes, quantitatively converging to a final result.

It was shown that self-consistency in this model requires that M_L be in the neighborhood of the Planck mass M_P $[(\hbar c/G)^{1/2} \sim 10^{19}$ GeV$/c^2]$,[15] probably on the high side. In addition, an estimate (of $\simeq 7$) for the value of the hadronic R in $e^+ e^-$ annihilations was derived. This estimate is consistent with present data,[16] and anticipates the discovery of some new quarks and/or heavy leptons.

II. THE MUON-ELECTRON SYMMETRY

In the context of this model, we are now ready to pursue the idea of Baker and Glashow,[17] that the μ-e mass splitting could be associated with a (second) symmetry breakdown. The symmetry in question is a permutation symmetry. As in I, it is assumed (as did Baker and Glashow) that the Lagrangian and Hamiltonian are of standard QED form, symmetric in the bare (massless) muon and electron wave functions. (The only known physical difference between the muon and electron is their rest mass.) Thus the operator P, permuting muon and electron, leaves the
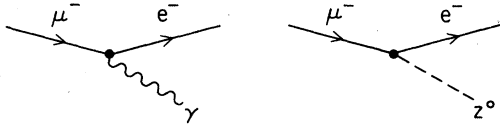
FIG. 3. Vertices forbidden by the conservation of the leptonic quantum number associated with Eq. (2).

Hamiltonian H invariant. That is,

$$[P,H]=0 . \tag{2}$$

It has been shown[18] that Eq. (2) results in a conservation law; the eigenvalues of P are constants of the motion[19] yielding a quantum number (± 1) which distinguishes muon from electron. This law forbids reactions containing vertices such as those shown in Fig. 3. In this regard, it is relevant to note that it has been established[20] that the process $\mu^{+} \to e^{+}\gamma$ is highly forbidden; its branching ratio is $<1.9 \times 10^{-10}$.

Bui-Duy, who has studied a model incorporating the idea of a permutation symmetry,[21] has shown that Eq. (2) holds for both symmetric and asymmetric solutions, and that no transitions are possible between these two regimes. He has pointed out that when a discrete symmetry, such as the permutation symmetry assumed here, is broken, one does not generate any Goldstone bosons, which have been shown to be associated with the breaking of a continuous symmetry.[6,22]

III. THE COUPLED EQUATIONS

Baker and Glashow pointed out[17] that the self-consistent, self-mass equations for the muon and for the electron are coupled through the masses of the fermions in the vacuum polarization loops. Since the initial Lagrangian is symmetrical in muon and electron, the resulting solutions for the electron mass and the muon mass will be of identical form, the muon mass being one of the parameters in the electron solution and vice versa. Therefore, if using this formulation one arrives at a solution for the electron mass

$$m_{e}=M(m_{\mu},\beta) , \tag{3}$$

where M is some functional form and β stands for all other parameters which enter the problem, then from the symmetrical formulation of the problem, the same solution will also apply to the muon, i.e.,

$$m_{\mu}=M(m_{e},\beta) . \tag{4}$$

The principle of self-consistency applied to the function M means that the appropriate solutions to the two-fermion mass-generation problem will be given at the intersection points of the lines

determined by Eqs. (3) and (4) plotted on a graph with m_{e} and m_{μ} as coordinate axes. Thus, from the permutation symmetry of the original Lagrangian, one expects that symmetric solutions with $m_{\mu}=m_{e}$ can be found.

The definition

$$\xi_{i} \equiv \frac{\alpha}{3\pi}\ln\frac{\Lambda^{2}}{m_{i}^{2}} , \tag{5}$$

where $\alpha \cong \frac{1}{137}$ is the fine-structure constant, enables the more convenient (dimensionless) parameters ξ_{i} to be used in place of m_{i}. As in I, Λ is placed at the ultraviolet cutoff. When convergence is obtained by means of a hard cutoff, Λ is just below M_{L}. When a (phenomenological form of a) physical cutoff is used, $\Lambda = M_{L}$.

Equation (5) enables us to replace Eqs. (3) and (4) by

$$\xi_{1}=F(\xi_{2})$$

and   (6)

$$\xi_{2}=F(\xi_{1}) ,$$

where the function F is appropriately derived from the function M, and notation of the parameters β is suppressed. The symmetric solutions are, of course, characterized by $\xi_{1}=\xi_{2}$.

In the case of interest in this paper, where the symmetry is a simple permutation symmetry, the disposition of the self-consistent solutions is easily visualized graphically by using what we shall call the mirror plot. In Fig. 4(a), $\xi_{1}=$ const (independent of ξ_{2}) is plotted, which is the result given by the usual second-order perturbation calculation [which uses only the first graph on the right-hand side of the equation shown in Fig. 2(a): no vacuum polarization and hence no coupling]. The same coordinate system, but where the roles of abscissa and ordinate are reversed (by reflection in the 45° symmetry axis), can also be employed for $\xi_{2}=$ const. Such a curve is also plotted in Fig. 4(a) where the intersection of the two lines (on the symmetry axis) yields the symmetric solution ($\xi_{1}=\xi_{2}$). As is seen below, when one goes to higher-order calculations, one gets a functional dependence of ξ_{1} upon ξ_{2} such that ξ_{1} diminishes as ξ_{2} increases. Curves schematically depicting this functional dependence are plotted in Fig. 4(b). Again, of course, the symmetric solution is on the symmetry axis.

Now as mentioned above, asymmetric solutions are also possible; one can imagine a functional dependence such that $\xi_{1}=F(\xi_{2})$ and $\xi_{2}=F(\xi_{1})$ intersect at points other than on the symmetry axis. These additional intersection points are also self-consistent solutions to the problem, but are asymmetric. In Fig. 4(c) a function F that
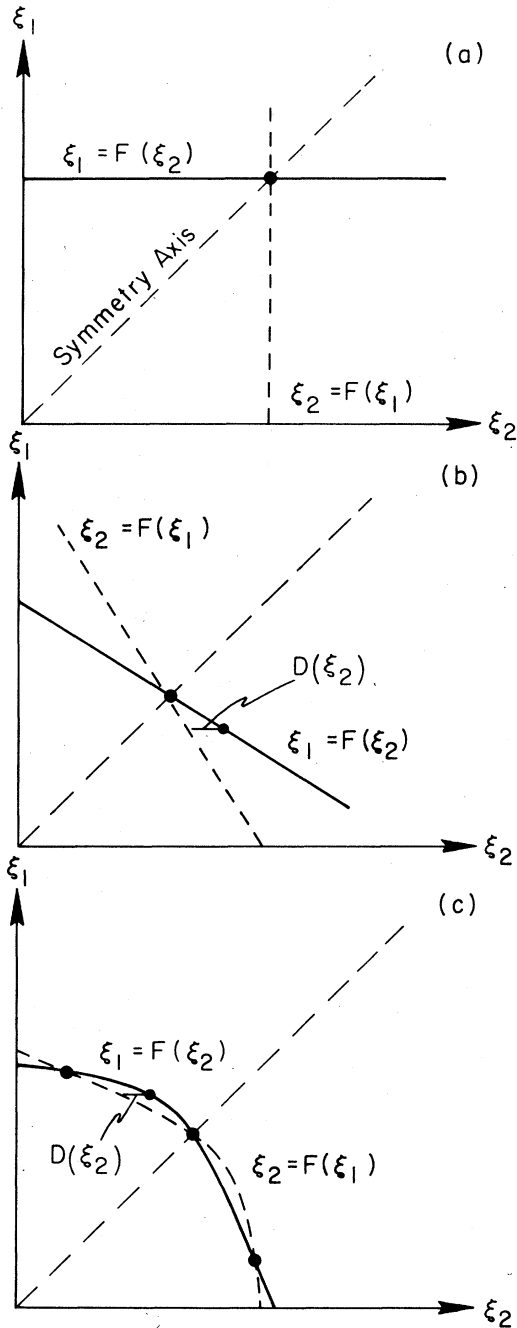
FIG. 4. Schematic plots of the mass parameters ξ_1 $=F(\xi_2)$, full curves, and $\xi_2=F(\xi_1)$, dashed curves, as symmetric functions of each other. The self-consistent solutions to the problem, which are located at the intersections of these curves, are indicated by the heavy dots. The symmetric solutions are on the 45° symmetry axis (all plots). In (c) the function F is such that there are also asymmetric solutions not on the 45° symmetry axis. A line segment indicating the quantity $D(\xi_2) \equiv F(\xi_2)$ $-F[F(\xi_2)]$ is drawn in (b) and (c). This quantity is equal to $\Delta(\xi_2)$ as defined in Appendix C. A point defining the appropriate ξ_2 to use as the function argument is indicated by the smaller dot on the $\xi_1 = F(\xi_2)$ line.

displays both symmetric and asymmetric solutions is plotted. These solutions may be stable, unstable, or degenerate (as defined below).

If there are self-consistent solutions, a simple criterion for their stability based upon self-consistency (rather than energy) may be developed.[23] One first imagines that a small perturbation temporarily moves the physical system away from the point of self-consistent solution. To represent this occurrence mathematically, one chooses a point (ξ_1', ξ_2') on the $\xi_1 = F(\xi_2)$ curve, say, near to but off of the intersection point in question. To test for (self-consistent) stability one then iteratively calculates $\xi_2 = F(\xi_1')$, $\xi_1 = F[F(\xi_1')]$, etc. One will be led by this procedure either toward the intersection point or away from it, independent of the side on which (ξ_1', ξ_2') was chosen. If such iterations lead one toward the intersection point, then that point shall be defined as stable; if they lead one away from the intersection point, then it shall be defined as unstable.

If we consider the symmetric solution, we see that if, on the symmetry axis

$$\frac{d\xi_1}{d\xi_2}=\frac{dF(\xi_2)}{d\xi_2} > -1, \qquad (7)$$

then such an iterative calculation will lead one toward the symmetric solution point, and that solution will be stable. Conversely, if $d\xi_1/d\xi_2$ < -1, the solution will be unstable. If $d\xi_1/d\xi_2$ $= -1$, the solution will be called degenerate.

This criterion for stability can be applied in general to any intersection on the mirror plot. At the intersection point (ξ_1, ξ_2) one needs only to determine the sign of the quantity

$$Q \equiv \frac{dF}{d\xi}\bigg|_{\xi=\xi_2} - \frac{1}{dF/d\xi}\bigg|_{\xi=\xi_1}; \qquad (8)$$

$Q > 0 \rightarrow$ stable ,

$Q < 0 \rightarrow$ unstable , $\qquad (9)$

and

$Q = 0 \rightarrow$ degenerate .

Equation (9) will be employed below as the criterion for stability. It can be seen that this criterion dictates that the stability of adjacent solutions in the mirror plot will alternate.

IV. DEGENERATE SOLUTIONS

As discussed in Sec. I, the symmetric solutions of the model in I were studied using a perturbation expansion in which the order n_γ denoted the number of photons, each photon carrying an approximation to its own vacuum polarization. Covergent expressions were obtained by analytically continu-

ing the functional form of the photon propagator beyond the Landau singularity and employing a "soft" physical cutoff at M_L. A Lorentz-invariant mathematical form was used to phenomenological-ly represent this cutoff, and the resulting integral was evaluated using the principal-value prescription.

We wish to maintain these features for the study of the asymmetric solutions. Unfortunately, the integral of the self-consistency equation using the Lorentz-invariant cutoff cannot be integrated in closed form. However, the slope of the function $F(\xi)$ is obtainable analytically. This slope reveals information about the stability of the solutions and, as it turns out, about the function $F(\xi)$ as well.

In Appendix B it is shown that in this formulation one obtains a slope of the form

$$\frac{dF}{d\xi} = \frac{d\xi_1}{d\xi_2} = -1 + \frac{R+2}{E'}, \tag{B23}$$

where E' is a divergent quantity going as $\lim_{\eta \to 0} 1/\eta$, and R represents the (effective) number of "ha-dronic"[24] pointlike fermions which couple to the photon. Thus, in the limit with $\eta = 0$,

$$\frac{d\xi_1}{d\xi_2} = -1. \tag{10}$$

It is pointed out in Appendix B that this result is independent of the details of the form of the (phenomenological) Lorentz-invariant cutoff; it need only be continuous across the Landau singularity, which on physical grounds is just what one would expect. It is also shown that this result is independent of the value of dimensionless parameter A', where A' is defined by Eq. (B12). Thus, assuming that (as indicated by the analysis in I) higher-order estimates of the leptonic self-mass merely alter somewhat the requisite value of A', Eq. (10) is valid to all orders of n_γ.

Since Eq. (10) is true in general, for $\xi_1 \neq \xi_2$ as well as for $\xi_1 = \xi_2$, in this approximation $\xi_1 = F(\xi_2)$ and $\xi_2 = F(\xi_1)$ plot as straight lines on the mirror plot, perpendicular to the symmetry axis. And since these lines must coincide at the point $\xi_1 = \xi_2$, they coincide everywhere. By the criterion of Eq. (9), therefore, in their limiting form, the solutions to the coupled, self-consistent self-mass equations are degenerate everywhere, forming a continuous set.

This degeneracy arises because, in essence, the slope calculation is dominated by divergence of the integrand at the Landau singularity. In the limit, A' is a function only of the sum $(\xi_1 + \xi_2)$, which occurs in the denominator of the vacuum polarization integral, and which specifies the location of the Landau singularity. While this

$(\xi_1 + \xi_2)$ symmetry is permutation symmetric, it goes beyond what is required in general from the original specification of permutation symmetry of the Lagrangian. It follows, then, that the $(\xi_1 + \xi_2)$ symmetry can be broken; as is discussed below, this leads to discrete solutions.

V. DISCRETE SOLUTIONS

One can see that if, as one approaches the limiting (degenerate) form of F, the $(\xi_1 + \xi_2)$ symmetry found above is broken, even infinitesimally, then the solutions to the coupled self-mass equation will be discrete. It follows that effects that are of negligible consequence for the symmetric solutions can be crucial for the asymmetric solutions; the degeneracy in the limiting form of F entails a sensitivity to any effect, no matter how small, that breaks the $(\xi_1 + \xi_2)$ symmetry.

This sensitivity precludes for this model the standard method for solving the coupled-mass problem: i.e., calculating order by order in n_e and examining the mirror plot of the resultant function F; since the Landau singularity is associated with the sum of an infinite number of vacuum polarization graphs, one anticipates that n_e would have to be taken to a very large number before features relevant to the possibilities of asymmetric solutions would appear. (Further-more, to be usable this very-high-order quasi-divergent calculation would have to be carried out to infinitesimal accuracy.) On the other hand, by using the limiting form as a reference solution and correcting it only by those effects which break the $(\xi_1 + \xi_2)$ symmetry, the prohibitive but irrelevant complications associated with the standard high-order calculations can be obviated.

For the purposes of analysis, the approach to the limiting form will be studied by imagining that our self-mass calculation is being performed in a cubical box of side B and volume $V = B^3$. In this situation, the (effective) number of fermion phase-space states N (including a factor 2 for both spin orientations) which are available for the inter-mediate-state integrations is $8\pi/3(B\Lambda/h)^3$ where h is Planck's constant. Thus for a large but finite box, N is a large but finite number. This step furnishes a (physically relevant) small parameter $1/N$ in which to expand the discrepancy Δ between the limiting or $(\xi_1 + \xi_2)$-symmetric form and the actual function F as it approaches this limiting form.

In Appendix C, by expanding Δ in a power series in $1/N$ [cf. Eq. (C5)], it is shown that indeed dis-crete solutions exist and that they are stable and independent of N as N (and $V) \to \infty$. [For Eq. (C5) to be valid it is, of course, required that the sym-metry-breaking effects that comprise Δ each

vanish like $1/N$ as $N \to \infty$; it is argued below that this is the case.] Therefore, in the limit $N \to \infty$, we recover the (appearance of a) continuous set of solutions, but at the same time have in actuality a set of stable discrete solutions. Subsequent numerical investigations discussed in Sec. VII show that, in fact, there is (independent of N) a region containing stable asymmetric solutions to the coupled self-mass problem.

VI. BREAKING THE $(\xi_1 + \xi_2)$ SYMMETRY

A. The $n_\gamma = 1$ approximation

In deciding where to look for $(\xi_1 + \xi_2)$-symmetry-breaking effects, we first recall that the coupling of the self-mass equations occurs only through the masses of the fermions in the vacuum polarization loops in the photon lines. We next note that the $(\xi_1 + \xi_2)$ symmetry has been shown to exist for the $n_\gamma = 1$ approximation (and evidently exists for all orders of n_γ). Thus, it is appropriate to study the $n_\gamma = 1$ approximation for $(\xi_1 + \xi_2)$ symmetry breaking. We argue further that the omission of consideration of the vertex function Γ^μ and the fermion propagator S_F' (see Fig. 1), which come into play in the higher-order approximations, does not lead to significant error because the Ward identity[25] dictates that renormalization effects due to these two functions cancel exactly to all orders. Any effects associated with photon lines internal in Γ^μ and S_F' must therefore (tend to mutally cancel and) be inferior to those which are found in the photon propagator D_F' already under direct scrutiny [see Figs. 1 and 2(a)] in the $n_\gamma = 1$ approximation. (An important exception to this conclusion is investigated in subsection C 2.)

In looking at the A' of Eq. (B13), which is derived from the $n_\gamma = 1$ self-mass integral, we anticipate that $(\xi_1 + \xi_2)$-symmetry-breaking effects can enter through: (1) the (lower) limits y_{min} and y_0, (2) possible variations of the functional form of the integrand over the range of integration, and (3) modifications of the integral in the neighborhood of $y_L = 1$. In the sections that follow, effects which break the $(\xi_1 + \xi_2)$ symmetry are indeed found which, respectively, fall into these categories: the fermion-mass-damping effect, the first Pauli effect, and the second Pauli effect.

B. The fermion-mass-damping effect

The fermion-mass-damping effect comes about because for small photon momentum vacuum polarization loops tend to become inoperative or damped out by the mass of the fermions in those loops. This damping, which is intuitively expected, derives from the one in the argument of

the logarithm in the expression for the one-loop vacuum polarization integral [see Eq. (A4)]. It can be seen from Eq. (B22) that this effect, which leads to a curvature or nonlinearity[26] in $F(\xi)$, is active when η of the principal-value prescription $\neq 0$, and furthermore that it goes to zero in proportion to η. This proportionality to η is important because through the second Pauli effect (subsection C 3, below) it leads to a proportionality to the parameter $1/N$, as is required for the validity of the expansion of Eq. (C5).

In Appendix A, the fermion-mass-damping effect is included in the hard cutoff approximation by dropping from the integral the contribution of loops of the ith type of fermion when the photon $K^2 < m_i^2$; expressions for A in this approximation are given there for four regions of the mirror plot. To obtain simpler calculations, these hard cutoff solutions will be used in the numerical analysis of Sec. VII, in which is investigated the structure of the solutions.

C. The Pauli exclusion principle

1. A brief review

Since in this model proper treatment of the Pauli exclusion principle plays a crucial role in the generation of mass splittings, it is useful to review briefly how the various electron self-mass calculations take the Pauli exclusion principle into account.

While the classical electromagnetic energy of an electron diverges linearly, Weisskopf[27] showed that a calculation using the Dirac positron theory diverges only logarithmically. This reduction in the severity of the divergence occurs because the presence of the electron in question perturbs the vacuum energy through the Pauli exclusion principle. In brief, vacuum fluctuations having an intermediate state identical to that of the original electron are precluded by the Pauli exclusion principle, and hence their energy must be subtracted from that of the unperturbed vacuum. This subtraction removes the most severe divergences associated with the "one-electron theory," leaving only a logarithmic ultraviolet divergence in the (second-order) self-mass calculation.

Following Weisskopf's approach, in time-ordered perturbation theory[28] one thus calculates the energy of the graph shown in Fig. 5(a) and subtracts the energy of the appropriate piece of the graph shown in Fig. 5(b). One of the beauties of the Feynman diagrammatic formulation is that the graph in Fig. 5(c) is numerically equal, but opposite in sign, to (the appropriate piece of) that in Fig. 5(b), enabling one to combine the time-ordered graphs in Figs. 5(a) and 5(c) [instead of
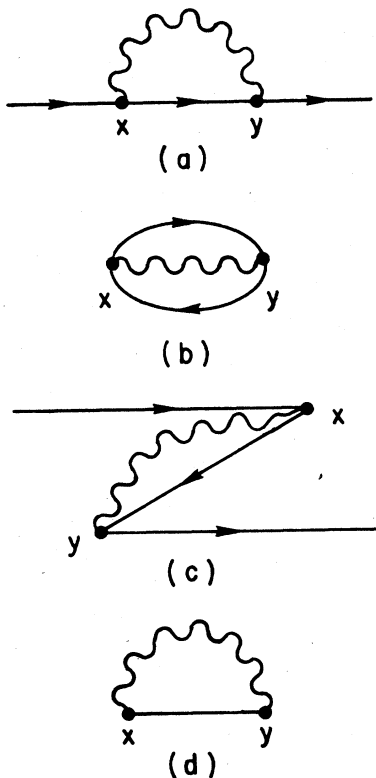
(a)

(b)

(c)

(d)

FIG. 5. Graphs of the electron propagator that are associated with the second-order electron self-mass. Graphs (a), (b), and (c) are time ordered with time increasing from left to right. (a) The electron emits a photon at x and reabsorbs it at y. (b) A vacuum fluctuation emits an electron-positron pair and photon at x and reabsorbs then at y. This graph is Pauli excluded when the electron is specified to be in the same state as the original electron whose self-mass is being calculated. (c) The vacuum at y emits, along with a positron and a photon, the final electron in the state of the initial electron. The photon and the positron annihilate with the initial electron at x. This graph is Pauli excluded because the initial and final electrons are in the same state at the same time. (d) Standard depiction of the second-order graph which is calculated by the Feynman rules to yield the second-order contribution to the proper electron self-mass. Points x and y are arbitrary, and the graph is evaluated by integrating x and y over all space-time.

those in Figs. 5(a) and 5(b)] to obtain the standard single second-order self-energy graph given in Fig. 5(d); it is simpler to forget about the vacuum bubble in Fig. 5(b) and just apply the Feynman rules to the graph of Fig. 5(d) to get the second-order contribution to the proper electron self-mass.[29]

It was emphasized by Feynman[30] long ago, in his discussion of the diagrammatic method for calculating QED processes, that the effects of the Pauli exclusion principle in the intermediate states are automatically taken into account. He recognized that whenever one used what are now known as the Feynman rules for calculating a graph (to some order in e) of a process, one erroneously included certain time-ordered pieces of that graph which actually should be omitted because of the Pauli exclusion principle. He pointed out, however, that this error does not really matter, because there is always another graph of the same order for the same process in which these very same Pauli-excluded pieces are likewise erroneously included, but with the opposite sign; and therefore, these calculational errors (which always come in pairs) always cancel. He showed in general that any calculation of a QED process which contains all graphs of a given order in e has in principle automatic and full compensation for the erroneously included (but Pauli-excluded) intermediate states; no errors are incurred in the final sum for that process and hence, when the Feynman rules are employed, no thought need be given to the operation of the Pauli exclusion principle in the intermediate states.

If follows that in an analogous manner, the Feynman rules properly (and to all orders) incorporate the Pauli-excluded time-ordered pieces of higher-order (self-mass) diagrams on the electron propagator as appropriate compensation for the Pauli-excluded pieces of the higher-order vacuum bubbles, whose energy is to be subtracted from that of the unperturbed vacuum. The pieces of the vacuum fluctuation bubbles which have no Pauli overlap with the self-mass diagrams may be ignored[30]; it has been shown in general[31] that in the perturbation expansion for the vacuum expectation value of time-ordered products of Heisenberg fields, which can be used to construct the S matrix for any process, the effect of these vacuum bubble graphs cancels out, leaving the perturbation expansion only in terms of the connected parts of the Feynman graphs.

2. The first Pauli effect

We recognize, then, that the proper method to determine the function F would be, order by order in e, to evaluate and sum all relevant graphs in the self-mass perturbation series. Using this procedure, by Feynman's compensation theorem, there would be no "effect" of the Pauli exclusion principle. But we have already noted that this method is not feasible; we have therefore used an expansion in which order denotes the number of photons. In this expansion, we do not get the benefits of this automatic "Feynman compensation" for certain Pauli-excluded states, because to be tractable the approximation selectively sums (what
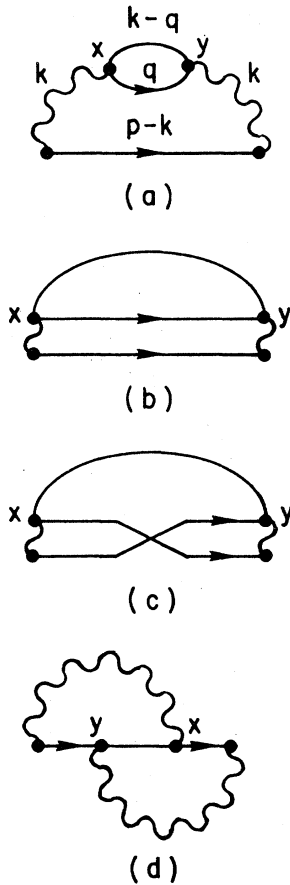
FIG. 6. This sequence of Feynman diagrams indicates the "Pauli overlap" of two self-energy graphs (fourth-order in e) of different topology. The intermediate-state interaction points x and y are labeled in each graph to clarify the relationships between the two types of graphs. The arrows on the fermion lines indicate the direction of fermion motion and the (intermediate-state) fermions to which the Pauli exclusion principle is to be applied. (a) Standard depiction of a one-photon diagram with one loop of vacuum polarization. Four-momentum p enters the diagram at the left; the loop momenta k and q circulate as indicated. (b) Diagram (a) deformed to depict the possibility that the two fermions in question can be in the same (Pauli-excluded) state. (c) Diagram (b) with the fermions interchanging. Since the two fermions are indistinguishable, diagrams (b) and (c) are indistinguishable. (d) Diagram (c) redrawn in the form of the standard depiction of a self-energy graph. The topology of this latter graph differs from that of the graph in (a), but these two graphs are seen to share exactly the same Pauli-excluded intermediate states. The signs of these two (Pauli-excluded) contributions differ due to the minus sign associated with the vacuum polarization loop.

we believe to be) the most significant graphs. These are the vacuum polarization graphs [Fig. 2(a)] which are of only one type of topology and

which give the Landau singularity, the major feature of our self-mass solution. Figure 6(a) gives an example of a graph included in the one-photon summation that has a Pauli-excluded piece whose (Feynman) compensation graph is omitted from the summation. We will call the effect of this deficiency the first Pauli effect for short.[32]

It is important to observe that this omission acts asymmetrically. That is, the graph in Fig. 6(d) which is missing in the one-photon expansion for δm, would compensate for an exclusion effect associated with leptons of type 1 (which by our convention is the lepton that we are "dressing"), but there is no equivalent (omitted) graph for leptons of type 2. Therefore, the omission of this and all other such graphs symmetrizes the contributions of the different fermion types to the vacuum polarization component of the self-mass calculation. Thus we see that the above found $(\xi_1 + \xi_2)$ symmetry in the limiting form of the function F is an artifact of our approximation, and not something which one expects to hold exactly from any general principle.

It is relevant to reiterate here that there are two options for graph calculation. On the one hand, while relying on the principle of Feynman compensation, one can (in principle) use the standard Feynman rules to calculate all of the graphs of a complete perturbation series to obtain the self-mass, or on the other hand, one is also (in principle) permitted to leave out the Pauli-excluded pieces calculating and summing only the Pauli-allowed pieces of these graphs. Feynman showed that these two options are numerically equivalent.

Since the standard method to determine the amount of $(\xi_1 + \xi_2)$ symmetry breaking is not feasible, the approach adopted here is to use the latter of the above options for graph calculation along with physical arguments to estimate directly the asymmetry induced into the $n_y = 1$ approximation by the first Pauli effect. To do this, we recall that our calculation is being performed in a box of volume V containing N phase-space states. Since one of these N states is already occupied by a lepton of type 1 (the lepton we are dressing), one expects the vacuum polarization integrals associated with leptons of type 1 to be slightly different from those associated with the lepton of type 2.

In order to estimate the magnitude of the piece of the vacuum polarization integral which should be Pauli excluded, we must examine the relationship between the fermion momentum in a typical loop and that along the line of the lepton being dressed. The Pauli exclusion principle will apply when two like fermions are in the same inter-

mediate state. In the diagrams that are included in the one-photon estimate $\delta m^{(1\gamma)}$, this relationship is straightforward [looking at Fig. 6(a) shows that the Pauli exclusion condition is $q = p - k$]. But as pointed out above, the effect we are trying to estimate here involves all of the self-energy graphs, as schematically depicted in Fig. 1. As we attempt to go into finer detail and use more elaborate graphs, we see that this relationship involves more momenta of integration and quickly becomes prohibitively complicated.

The complicated physical motion which the set of higher-order graphs of the fermion propagator mathematically describes is called *Zitterbewegung*.[33] This *Zitterbewegung*, involving the fermions in the vacuum polarization as well as the original fermion line, in effect randomizes the relationship between the (instantaneous) momemtum in a given vacuum polarization loop and the (instantaneous) momentum being carried along the original fermion line. That is, when one looks into the details of the propagators, one sees that the state that the original fermion excludes by its mere presence is, in effect, uncorrelated in momentum with the states in the vacuum polarization loops. Thus, the Pauli-excluded state (for type-1 leptons) may be accounted for by removing it with an appropriate random probability from the N available phase-space states over which the loop sums (integrals) are taken.

The probability of removal can be represented by an effective probability density function $p_1(y)$, which then yields a factor $[1 - p_1(y)]$ in the vacuum polarization integrand. The variable y is defined by Eq. (B2). The notion of *Zitterbewegung* leads one to expect that the distribution $p_1(y)$ will be very broad and relatively flat, ranging out to the Landau momentum. We can represent this $p_1(y)$ by a (Fourier) series expansion. The zeroth order or *dc* term of this expansion will equal $1/N$, since $\int p_1(y) dy = 1/N$, with higher-order terms causing $p_1(y)$ to fall off to zero at large y.

Keeping only the zeroth-order term and dropping the higher-order contributions to the vacuum polarization integral enables a straightforward zeroth-order estimate of the first Pauli effect. We merely associate a factor

$$1 - \epsilon_1 \cong 1 - \frac{1}{N} \qquad (11)$$

with each vacuum polarization loop in which a fermion of type 1 circulates. It is easy to see that this modification, applied to the self-mass series depicted in Fig. 2(a), will give a perturbation series which sums to yield

$$\left[1 - (1 - \epsilon_1) \frac{\alpha}{3\pi} \ln \frac{K^2}{m_1^2} - \frac{\alpha}{3\pi} \ln \frac{K^2}{m_2^2} - \frac{R\alpha}{3\pi} \ln \frac{K^2}{m_3^2} \right] \qquad (12)$$

as the vacuum polarization denominator.

At first it might be surprising that the pieces of the graphs in Γ^μ and S_F' brought into play by this accounting for the Pauli exclusion principle have the same functional form as does (the sum of) the vacuum polarization graphs; that means that they contain (infinitesimal) non-Borel summable components (entering with like, rather than alternating, sign). But then this must be the case because the graphs with which they share a Pauli-excluded overlap are non-Borel summable, a fact which brings about the Landau singularity in the vacuum polarization integral (which accounts for the electric charge renormalization). Since this singularity is not manifest in the individual graphs but rather is evident only by their (non-Borel) summation, then, too, the components of Γ^μ and S_F' that are associated with the first Pauli effect would be manifest in the standard method with the above functional dependence (proportional to ϵ_1) only by summation. Thus, until one has the ability in the standard approach to (exactly) calculate and sum to very high order all of the graphs in the self-mass series, what is here called the first Pauli effect would not be revealed; the infinitesimal non-Borel summable part would be totally obscured at the level of the individual graph by the much larger Borel summable parts.

Equation (12) tells us that the first Pauli effect (re vacuum polarization loops) acts like an infinitesimal charge renormalization of the lepton of type 1, but Eq. (11) tells us that as the normalization box size goes to infinity, the first Pauli effect goes to zero as $1/N$, eliminating in the limit this charge renormalization. Nevertheless, as the E' of Eq. (B23) becomes large (because of the Landau singularity) Eq. (12) leads to a slope at the symmetry point of

$$\left. \frac{d\xi_1}{d\xi_2} \right|_{\xi_1 = \xi_2} = -1 - \epsilon_1 < -1 . \qquad (13)$$

That is, inclusion of this correction to the limiting form yields a symmetric solution that is discrete and unstable.

3. The second Pauli effect

The second Pauli effect is a saturation phenomenon associated with graphs of extremely high order. It comes about because we are using a physical cutoff at the Landau mass and are performing our calculation in a finite box.

It is clear that when we perform our analysis in the box of volume V, graphs of order $\gg N$ will have so many fermion lines that they must be comprised (almost) entirely of Pauli-excluded pieces. It follows, therefore, that by taking the point of view of the second option for graph cal-

culation, these graphs may be entirely omitted from the perturbation summation. That is, among these graphs (for some specified order $\geq N$) it is appropriate, because of the Pauli exclusion principle, just to truncate the perturbation series.[34]

For the purposes of estimation of this second Pauli effect we shall truncate the summation of graphs associated with the one-photon estimate when the power of α exceeds $N' = (R+2)N$; for many loops and high momentum the fermion loops will be equally populated by the $(R+2)$ different types of fermions, giving the additional factor[35] of $(R+2)$. One expects there to be a factor (of order unity) correcting the (effective) location of this saturation point; this is included in the list of errors below.

In the hard cutoff solution, this Pauli saturation effect can be taken into account simply by subtracting a second infinite series, which starts at $n = N'$, and then resumming: i.e.,

$$\frac{1}{1-y} \to \sum_{n=0}^{\infty} y^n - \sum_{n=N'}^{\infty} y^n = \sum_{n=0}^{\infty} y^n - y^{N'} \sum_{n=0}^{\infty} y^n = \frac{1-y^{N'}}{1-y}.$$

(14)

In the one-photon approximation, the Pauli saturation effect will become active at the value $y = 1 - 1/N'$, which is infinitesimally below the Landau singularity. Therefore, with a hard cutoff, this Pauli effect will be negligible; while we expect that A is a number of order unity, even if it is large, the self-consistent value for the hard cutoff will fall well below the value $y = 1 - 1/N'$.

From the above discussion, it follows that when we include a Lorentz-invariant cutoff at M_L and a momentum integration to infinity, for a finite-sized normalization box, this second Pauli effect will prevent the photon propagator from actually diverging at the Landau singularity; the propagator becomes very, very large at $K^2 = M_L^2$, but nevertheless remains finite, $\sim N'$. For $y < 1$, this result follows directly from Eq. (14); there are N' terms in the summation, each of which for $y = 1^-$ equals unity.

We now assume that the influence of this Pauli saturation effect upon behavior of the (analytically continued) photon propagator for $y > 1$ is symmetric. That is, the negative excursion of the propagator at $y = 1^+$ is also finite and $\sim N'$. Such an assumption is required for the mathematical stability of the principal-value prescription; its basis could be sought either in a physical description of features on the scale of the Landau length[36] or in mathematical analysis.[37] In either case it can be taken into account by setting the η in Eq. (B26) to a constant rather than taking it to zero. From the discussion associated with Eq. (14) we

have seen that this constant should be $\sim 1/N'$.

One can see that the second Pauli effect acts in the opposite sense to the first Pauli effect, tending to stabilize the symmetric solution (increasing the slope $d\xi_1/d\xi_2$). Correcting for both Pauli effects, one rewrites Eq. (13) as

$$\left. \frac{d\xi_1}{d\xi_2} \right|_{\ell_1 = \ell_2} = -1 - \epsilon_1 + \epsilon_2 ;$$

(15)

both ϵ_i are greater than zero and of comparable size.

We assert that while there would, of course, be no Pauli effects, as such, in a standard self-mass calculation, because of the equivalence of the two options for graphs calculation, the slope of the function F determined by such a calculation in a finite box to sufficiently high order would still be given by Eq. (15). As the normalization volume V is taken to infinity, N goes to infinity and these Pauli effects become infinitesimal as $1/N$, effectively vanishing. The Landau singularity of the photon propagator then recovers its (limiting) $1/(1-y)$ form.

For the purposes of the numerical study in Sec. VII, it is useful to rewrite Eq. (15) as

$$\left. \frac{d\xi_1}{d\xi_2} \right|_{\ell_1 = \ell_2} = -1 + \epsilon_2(1 - \rho) ,$$

(16)

where

$$\rho \equiv \frac{\epsilon_1}{\epsilon_2}.$$

(17)

It will be seen that the structure of the solutions is a function only of the ratio ρ, in which, as required by Eq. (C5), the value of N cancels. This cancellation enables one to make an estimate of the leptonic mass splitting.

VII. NUMERICAL ANALYSIS

A. Mathematical formulation

An analysis which includes the above features, which vanish as $1/N$, faces certain practical difficulties; self-consistent integral equations incorporating these features cannot be solved analytically in closed form, and the computer cannot deal with infinitesimal quantities. There is a computational approach, however, which can be used to circumvent these difficulties. This approach is based upon the results of Appendix C which show that for large N, the locations of the self-consistent solutions are independent of the actual value of N. This means that we can perform an analysis using a value of N tractable to computer calculations obtaining the same results that would be derived in the limit as N goes

to infinity.

It is possible to carry through this approach using the results in Appendix A, which employ the hard cutoff; parameters in that approximation are used to simulate the Pauli effects, but with a tractable (effective) value of N. Full self-consistency, however, must be given up when the hard cutoff results are employed. That is, both the mean mass parameter $\bar{\xi} \equiv (\xi_e + \xi_\mu)/2$ and the mass splitting $\xi_e - \xi_\mu$ cannot be determined at the same time. This is not a serious drawback since in principle $\bar{\xi}$ can be determined from the self-consistent symmetric solutions, which are not influenced by the infinitesimal Pauli effects.

We recall that in I, R was determined by using the self-consistency condition $\delta m/m = 1$, setting the value of A', of Eq. (34I), according to the order of the approximation. On the other hand, using the hard cutoff solution precludes a self-consistent relationship between A and R, leaving them both as free parameters. As free parameters A and R can be used to set the value of the slope at the symmetry point (mainly through A), and the value of $\bar{\xi}$ (mainly through R). $\bar{\xi}$, assumed to be already determined from the symmetric solutions, thus determines the value of R to be used in this numerical study. It can be seen from Eq. (B27) that setting the slope at the symmetry point in this way simulates the second Pauli effect and is like choosing an effective value of N for the problem. With these steps taken, a variation of the parameter G ($1 - G$ goes like ϵ_1 of the first Pauli effect) will now yield a parametric study of the structure of the solutions.

B. Structure of the solutions

This analysis has been carried out using Eqs. (A7)–(A10). The values of the parameters employed are $A = 1$ for convenience, $\xi_3 = 0.063\,45$ (this is equivalent to $m_3 = 20\,\mathrm{GeV}/c^2$ for $\Lambda = M_P$; Λ is arbitrarily set to M_P rather than self-consistently determined. As will be seen below, other errors will completely dominate the one introduced by this choice[38]) and $R = 13.377$ to yield $\bar{\xi} = 0.0757$ [equivalent to $\bar{m} = (m_e m_\mu)^{1/2}$ for $\Lambda = M_P$]. The choice for ξ_3 is slightly coupled to the choice for R, but variations of ξ_3 do not qualitatively affect these results and hence are unimportant here. (It will be seen below that calculational errors and unknown non-QED physics preclude a quantitatively convincing calculation.) The choice of $A = 1$ fixes the amount of the second Pauli effect, and via Eqs. (16) and (17) effectively sets a scale for the first Pauli effect. It is the relative size of the two Pauli effects as given by the parameter ρ which is relevant to the structure of the solutions; the N dependence cancels out.
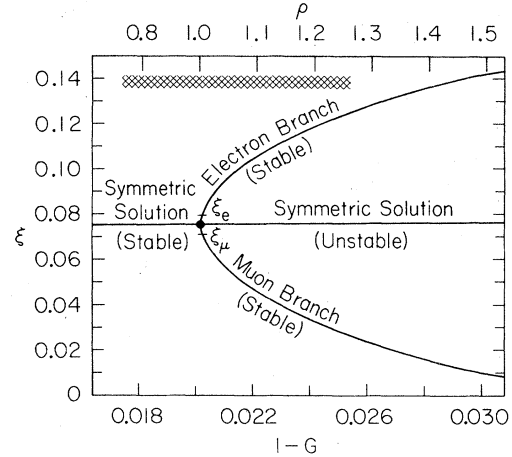

FIG. 7. A representative plot of the self-consistent solution points in the parameter ξ of the self-consistency equations versus $1 - G$ along the lower abscissa. As discussed in Sec. VII, this plot simulates the inclusion of the two Pauli effects. A scale for ρ, the ratio of these two effects, is indicated along the upper abscissa. For $1 - G$ close to zero, there is only a stable symmetric solution [corresponding to the mirror plot in Fig. 4(b)]. As $1 - G$ increases, a trifurcation point is reached, indicated by a dot at $(1 - G) = 0.020\,14$. At this point the two Pauli effects are equal, defining the point $\rho = 1$, and the solutions are degenerate. Beyond this point there are three solutions, an unstable symmetric one and two stable asymmetric ones [corresponding to the mirror plot in Fig. 4(c)]. The more massive of these stable asymmetric solutions is labeled "muon branch" and the less massive "electron branch." A range in which the estimate of ρ is expected to fall (see Table I) is indicated by the cross hatching along the upper abscissa. This range includes $\rho = 1.005\,46$ for which the observed muon and electron masses are stable asymmetric solutions at $\xi_\mu = 0.0716$ and $\xi_e = 0.0798$ are indicated.

The results, plotted in Fig. 7, reveal the following structure. When $(1 - G) = 0$, the first Pauli effect is null. In this case, as we anticipate from the above discussion, there is one solution (since $E' < \infty$), a stable symmetric one [as depicted in Fig. 4(b)]. As $(1 - G)$ is increased (i.e., G is diminished) a degenerate or trifurcation point is reached; this point represents equality of the two Pauli effects at the symmetry point, defining the location of $\rho = 1$, and hence the scale of the abscissa in terms of ρ. As $(1 - G)$ is increased yet further (the first effect now exceeding the second), one enters a region having asymmetric as well as symmetric solutions [as depicted in Fig. 4(c)]. By the criterion of Eq. (9) the asymmetric solutions are stable and the symmetric ones unstable.

The structure of the solutions given in Fig. 7 can be shown to be independent of the selection

of the effective value of N. That is, increasing the value of A merely moves the trifurcation point closer to $G = 1$, rescaling the abscissa and at the same time the "parabola" of the asymmetric solutions. This assertion has been numerically verified on the SLAC IBM 360/91 computer to the extent possible (quadruple precision, going up to $A = 3$). Several values of A were selected and the analysis repeated. Independent of the value of A, relative to the trifurcation point, the general structure of the solutions as a function of ρ remained invariant; only the overall scale of the abscissa was changed, and taking this scale change into account, the parabolas of the asymmetric solutions were (essentially) congruent. The fact that values of A in the range $1 < A < 3$ (which is equivalent to the range $60 < N < 5.3 \times 10^7$) yield solutions with the same structure indicates that $A = 1$ already simulates a value of N in the asymptotic region.

C. Estimate of the splitting

To estimate the splitting $\xi_e - \xi_\mu$ we must determine ρ from the relative magnitudes of ϵ_i. As indicated in Sec. VI C 2, ϵ_1 may be approximated by $1/N$. In Appendix B, we see from Eq. (B27) that the one-photon estimate for ϵ_2 gives

$$\epsilon_2 = \frac{1}{2L(1)Nf}, \tag{18}$$

where $L(1)$ is the value of the phenomenological Lorentz-invariant cutoff at the Landau singularity ($y = 1$), and f is a factor expected to be of order unity. Using Eq. (18) gives the estimate

$$\rho = \frac{1/N}{[2L(1)Nf]^{-1}} = 2L(1)f. \tag{19}$$

Several possible functions $L(y)$ are listed in Table I, with their value at $y = 1$, i.e., at $K^2 = \Lambda^2$, where K^2 is the Euclidean four-momentum defined in Appendix A. While these different functions do not yield significantly different results for the symmetric solutions found in I, the asymmetric solutions under study here are extremely sensitive to the value of $L(1)$. The range of ρ associated with the span of $L(1)$ of these functional forms is

TABLE I. Some phenomenological cutoff functions.

$L(y)$	$L(1)$	$\rho = 2L(1)$	Note
$1 - e^{-\Lambda^2/K^2}$	0.632	1.264	Used in I, Eq. (34I)
$\dfrac{1}{\exp\left(\dfrac{K^2}{\Lambda^2} - \dfrac{\Lambda^2}{K^2}\right) + 1}$	0.5	1.000	A pseudo-Fermi functional form
e^{-K^2/Λ^2}	0.368	0.736	Standard exponential

plotted in Fig. 7. Since there is already a range of ~2 uncertainty in ρ due to the value of $L(1)$, no additional error is included for the factor f, which has been set to unity. As indicated in Fig. 7, it can be seen that this span of ρ includes $\rho = 1.005\,46$, which yields the observed $\xi_\mu = 0.0716$ and $\xi_e = 0.0789$.

D. Discussion of errors

Errors in the estimated m_μ/m_e enter in two places: (1) the factors relating the ϵ_i to N^{-1} and (2) the conversion of the estimated value of ρ (using the solution structure depicted in Fig. 7) into $\xi_e - \xi_\mu$, which by exponentiation yields m_μ/m_e. The former category includes estimates, via phase-space arguments, of the specific influence of the Pauli-excluded pieces of the Feynman diagrams, the influence of the strong interactions of the hadronic pointlike particles,[39] and the unknown physics associated with the phenomenological function $L(y)$. The latter category includes factors which change the shape of the parabola of Fig. 7, such as the modification of the vacuum polarization by the strong interaction, the representation of masses of the heavier fermions by m_3, and the approximation used to represent the fermion-mass-damping effect.

Since the span of reasonable values of ρ includes both regions, i.e., stable symmetric and stable asymmetric solutions, until more is known about the phenomenological function $L(y)$, one cannot estimate the mass splitting using this model. Furthermore, the estimate of the mass splitting is very sensitive to the estimate of ρ. For example, the upper limit of the range $\rho = 1.26$ is only about 25% away from the "correct" value, yet at this point one has $m_\mu/m_e = 8 \times 10^{26}$. It is easy to see that this extreme sensitivity of the deduced mass ratio m_μ/m_e to small changes (errors) in the estimate of ρ is because m_μ/m_e is determined by the exponentiation of the logarithmic quantities ξ_i; specifically, from the curve in Fig. 7 one can deduce that to determine m_μ/m_e to an accuracy of 10% requires that the estimate of ρ be accurate to ~2 ppm. Thus, now and for some time to come, the unknown non-QED physics will in this model preclude a satisfactory estimate of m_μ/m_e, even though it may be possible (in principle given sufficient effort) to reduce the QED associated errors to an acceptable level. On the other hand, one can make an extrapolation of the model in which these difficulties are minimized.

VIII. EXTRAPOLATION OF THE MODEL

If the mass splitting of the muon and electron are generated by the breakdown of a permutation

TABLE II. Heavy-lepton-mass predictions for several models.

Model	Mass predictions[a]	Comments
Tennakone and Pakvasa[b]	22, 4554,...	Discrete scale transformations
Rosen[c]	1.915, 15.67,...	QED self-mass formulation including gravitation
Blaha[d]	31.52,...	Wave equation with a relativistic potential
Bjorken[e]	~10	Logarithm of mass is a smooth function
Pais[f]	~380	Quark-lepton mass relationship extending "standard model"
Barut[g]	1.786 08, 10.2937,...	Quantized magnetic self-energy
Krolikowski[h]	25.5, 455,...	Second-order difference equations for mass and charge
Caldirola[i]	0.1056, 1.794, 21.58,...	"Chronan" hypothesis including "internal" states
This model	~380	QED self-mass formulation with symmetry breaking between pairs of leptons

[a] In GeV/c^2.
[b] Reference 42.
[c] Reference 43.
[d] Reference 44.
[e] Reference 45.
[f] Reference 46.
[g] Reference 47.
[h] Reference 48.
[i] Reference 49.

symmetry as analyzed above, then the simplest assumption is that (charged) leptons must come in pairs. If there is such a permutation symmetry between e and μ, then by extrapolation there will also be one between the τ and a yet heavier lepton[40] which we here call the T. While we have seen that the splittings within a pair cannot be calculated with a sufficient degree of accuracy, one expects the computational and other errors associated with each pair to be similar. Thus, anticipating that to first order the ratios of the masses in each pair are the same, we use the observed μ-e mass ratio to make our extrapolation

$$\frac{m_\mu}{m_e} \simeq \frac{m_T}{m_\tau}, \qquad (20)$$

which yields $m_T \simeq 380$ GeV/c^2. This estimate[41] is compared in Table II to heavy-lepton mass estimates given by some other models.

IX. SUMMARY AND CONCLUSIONS

This paper continues the study of a model based upon the suggestion of Baker and Glashow that the μ-e mass splitting might be associated with a symmetry breaking in the QED self-mass formulation. The initial paper, I, developed a self-consistent formulation for the (leptonic) self-mass and considered the symmetric solutions. This paper considers the possibility of asymmetric solutions. The symmetry that is broken to yield these asymmetric solutions is a permutation symmetry. This broken permutation symmetry introduces in a natural way a quantum number which distinguishes muon from electron, and which forbids μ-e transitions. It is noted that the experimental upper limit on the branching ratio for $\mu \to e\gamma$ is indeed very, very small ($< 1.9 \times 10^{-10}$).

Here, as in I, we have seen that vacuum polarization plays a crucial role in the physics of this model for the generation of leptonic masses and their splittings. In I, it was accepted as part of the model that vacuum polarization led to the existence of a (Landau) singularity in the photon propagator. Here, as in I, this difficulty was controlled by assuming that the photon propagator has the same functional form above M_L as it does

below (where it was determined by the summation of a perturbation series) and that there was a physical cutoff at M_L.

It was shown that in this formulation the Landau singularity dominates the self-consistent, self-mass calculation yielding a (continuous) set of degenerate solutions. These degenerate solutions manifest in their limiting form what we call a $(\xi_1 + \xi_2)$ symmetry and are sensitive to effects that break this symmetry, no matter how small. Because of this sensitivity, it was shown that two new aspects, not considered in I, are significant. These aspects, also intimately associated with the vacuum polarization, are called the fermion-mass-damping effect and the Pauli effects. Their inclusion was shown to break the $(\xi_1 + \xi_2)$ symmetry as one approaches the limiting form and change the continuous set of solutions into a discrete set that included both symmetric and asymmetric parts.

The structure of these solutions was investigated, and a method for estimating mass splitting was given. It was shown that this estimate is extremely sensitive to numerical errors. While these errors unfortunately stem in large measure from non-QED physics and are indeed much too large to permit a quantitatively convincing estimate, this difficulty should not obscure the qualitative fact that this model does have the possibility of asymmetric solutions compatible with the observed μ-e ratio. In mitigation it is perhaps worthwhile to note that there are well-known physical systems which also exhibit extreme sensitivity to certain parameters, e.g., those involving critical phenomena or phase transitions. It should also be remarked that while this model is extremely sensitive to intrinsic computation errors, it cannot be said that the correct μ-e mass ratio can result only by an exquisite cancellation of two opposing effects; $\rho = 1 + (3/4)\alpha$ gives (a good approximation to) the observed m_μ/m_e, and α, while small, is not vanishingly small.

Ultimately, of course, one hopes for an improved experimental knowledge of the fermion spectrum and theoretical understanding of the interactions to enable calculations of adequate accuracy. Until such time, it appears that the best test of this model is a search for the yet heavier lepton predicted by an extrapolation of the model at ~380 GeV/c^2. This prediction is less subject to the difficulties mentioned above because it derives from an already observed mass ratio, which should afford a significant compensation for the intrinsic errors. Such a search would at the same time test the lepton mass predictions of several other models (see Table II) which fall within the capabilities of coming generations of accelerators.

Finally, it is interesting to note that, should this model be relevant to describe the μ-e mass splitting, the fact that the observed μ-e mass ratio is on the order of α appears to be fortuitous, rather than the consequence of a simple, direct relationship to the magnitude of α. In this model, one would not expect α to play a direct role in the mass ratio (i.e., $m_e \sim \alpha m_\mu$) since both leptons acquire their masses self-consistently and "at the same time."

APPENDIX A: A GENERALIZATION OF THE ONE-PHOTON ESTIMATE OF THE SELF-MASS

In Appendix A of I, a one-photon estimate of the leptonic self-mass $\delta m^{(1\gamma)}$ was derived. The usual Feynman rules of QED and the notation of Bjorken and Drell[50] were used to write down the integrals associated with the graphs shown in Fig. 2(a). It was assumed that, participating in the polarization of the vacuum, there are (an effective number) R other pointlike particles in addition to the two leptons. A Wick rotation[51] was employed to convert these integrals from expressions in Minkowski space (k_μ, $\mu = 0$, 1, 2, 3) to ones in Euclidean space. The substitutions to effect this rotation are

$$k_0 = iK_4, \quad k_j = K_j, \quad \text{and} \quad k^2 = -K^2, \tag{A1}$$

where $j = 1, 2, 3$ and $i = \sqrt{-1}$. As discussed in I, the infrared problems were ignored, and only the leading terms in the ultraviolet cutoff were kept. The resulting expressions were then summed.

Since the interest in I was in the symmetric solutions, all $(R + 2)$ masses were set equal to m, yielding the one-photon estimate

$$\delta m^{(1\gamma)} = \frac{9m}{4(R + 2)} \ln\left[\frac{1}{1 - (R + 2)(\alpha/3\pi)\ln(\Lambda^2/m^2)}\right].$$

$$\tag{A13I}$$

(The I appended to an equation number indicates that that equation is taken from I.) Λ in this equation is a hard cutoff just below the Landau singularity. From Eq. (A13I) the dimensionless quantity

$$A \equiv \frac{9}{4(R+2)} \ln\left[\frac{1}{1-(R+2)(\alpha/3\pi)\ln(\Lambda^2/m^2)}\right]$$

(A14I)

was defined.

One can easily generalize this result to apply to the case of differing fermion masses. Using the definition

$$\xi_i \equiv \frac{\alpha}{3\pi} \ln \frac{\Lambda^2}{m_i^2} ,$$

(A2)

where $i = 1$ or 2 stands for the (two) leptons and $i = 3$ subscripts an effective "threshold" mass (for the contribution of the R "hadronic" pointlike particles as a set), Eq. (A13I) becomes

$$\delta m_1^{(1\gamma)} = \frac{9m_1}{4(R+2)} \ln\left[\frac{1+(R+1)\xi_1-\xi_2-R\xi_3}{1-\xi_1-\xi_2-R\xi_3}\right] .$$

(A3)

Equation (A3) uses the convention that $i = 1$ represents the lepton acquiring the self-mass and $i = 2$ the lepton whose mass is specified as a parameter in the expression for δm_1.

An improvement upon this approximation can be made by noting that in the expression for the vacuum polarization due to one fermion loop,[52]

$$\frac{2\alpha}{\pi} \int_0^1 z(1-z)dz \ln\left[1+\frac{z(1-z)K^2}{m_i^2}\right] ,$$

(A4)

the argument of the logarithm is always greater than unity (when we work in our symmetric Euclidean four-space), and hence the logarithm in Eq. (A4) is always positive. But, for small K^2, $\ln[\ ] \to \ln 1 = 0$. This fact can be (approximately) taken into account by dropping the contributions of the loops of the ith fermion when

$$K^2 < m_i^2 ,$$

(A5)

which is in accord with intuition. In the text this effect is called the fermion-mass-damping effect.

When employing Eq. (A5), there are four regions of interest in the mirror plot (see Fig. 4) defined as follows:

Region I: $\xi_1 \leqslant \xi_3 < \xi_2$ or $m_1 \geqslant m_3 > m_2$,

Region II: $\xi_3 < \xi_1 \leqslant \xi_2$ or $m_3 > m_1 \geqslant m_2$,

Region III: $\xi_3 \leqslant \xi_2 < \xi_1$ or $m_3 \geqslant m_2 > m_1$,

Region IV: $\xi_2 < \xi_3 < \xi_1$ or $m_2 > m_3 > m_1$.

(A6)

The results of the self-mass integrations are recorded below. The quantity G, which is to account for the first effect of the Pauli exclusion principle (discussed in Sec. VIC), equals $(1-\epsilon_1)$; cf. Eq. (12). G is unity when this effect is ignored.

Region I:

$$\frac{9m_1}{4(R+G+1)} \ln\left[\frac{1+(R+1)\xi_1-\xi_2-R\xi_3}{1-G\xi_1-\xi_2-R\xi_3}\right] ,$$

(A7)

essentially the same as Eq. (A3).

Region II:

$$\frac{9m_1}{4(G+1)} \ln\left[\frac{1+\xi_1-\xi_2}{1-G\xi_1-\xi_2+(G+1)\xi_3}\right] + \frac{9m_1}{4(R+G+1)} \ln\left[\frac{1-G\xi_1-\xi_2+(G+1)\xi_3}{1-G\xi_1-\xi_2-R\xi_3}\right] .$$

(A8)

Region III:

$$\frac{9m_1}{4G} \ln\left[\frac{1}{1-G\xi_1+G\xi_2}\right] + \frac{9m_1}{4(G+1)} \ln\left[\frac{1-G\xi_1+G\xi_2}{1-G\xi_1-\xi_2+(G+1)\xi_3}\right] + \frac{9m_1}{4(R+G+1)} \ln\left[\frac{1-G\xi_1-\xi_2+(G+1)\xi_3}{1-G\xi_1-\xi_2-R\xi_3}\right] .$$

(A9)

Region IV:

$$\frac{9m_1}{4G} \ln\left[\frac{1}{1-G\xi_1+G\xi_3}\right] + \frac{9m_1}{4(R+G)} \ln\left[\frac{1-G\xi_1+G\xi_3}{1-G\xi_1+(R+G)\xi_2-R\xi_3}\right] + \frac{9m_1}{4(R+G+1)} \ln\left[\frac{1-G\xi_1+(R+G)\xi_2-R\xi_3}{1-G\xi_1-\xi_2-R\xi_3}\right] .$$

(A10)

Analogous to Eq. (A14I) one may now define a more general form for A as the respective expressions obtained from Eqs. (A7), (A8), (A9), or (A10) divided by m_1. These expressions for A are the appropriate dimensionless quantities to use when the fermion masses are not assumed to be the same.

APPENDIX B: SOME SLOPE CALCULATIONS

The hard cutoff integral for the dimensionless parameter A (defined in Appendix A) which would be associated with Eq. (A3) can be expressed in the form

$$A = \frac{9}{4(R+2)} \int_{y_{min}}^{y_{max}} \frac{dy}{1-y} ,$$

(B1)

where, analogous to Eq. (31I),

$$y = \frac{\alpha}{3\pi}\ln\frac{K^2}{m_1^2} + \frac{\alpha}{3\pi}\ln\frac{K^2}{m_2^2} + \frac{R\alpha}{3\pi}\ln\frac{K^2}{m_3^2} \, , \tag{B2}$$

$$y_{\min} = -(R+1)\xi_1 + \xi_2 + R\,\xi_3 \, , \tag{B3}$$

$$y_{\max} = \xi_1 + \xi_2 + R\,\xi_3 \, , \tag{B4}$$

and the ξ_i are defined by Eq. (5). Since $i=1$ is the lepton acquiring the (self-consistent) self-mass and $i=2$ represents the "parametric" lepton, we are studying $\xi_1 = F(\xi_2)$; in particular $d\xi_1/d\xi_2 = dF/d\xi$.

We now recall that Eq. (1) for the $n_\gamma = 1$ approximation yields the self-consistency condition $A - 1 = 0$. It was shown in I that in like fashion higher-order approximations lead to the condition $P(A) = 0$, where n_γ is the highest power of A in the polynomial expression $P(A)$. Thus, in general, the self-consistency condition leads to the specification that $A = $ constant, where the constant is determined according to the order n_γ of the approximation. (In I it was shown that for $n_\gamma = 2$, $A = 1.3136$.) Therefore, the total differential of A, $dA = 0$, independent of n_γ.

Now the quantity dA can be calculated without actually integrating. Consider the formula[53]

$$\frac{d}{dc}\int_a^b f(y,c)dy = \int_a^b \frac{\partial}{\partial c}f(y,c)dy$$
$$+ f(b,c)\frac{db}{dc} - f(a,c)\frac{da}{dc}. \tag{B5}$$

Since the integrand of Eq. (B1) has no functional dependence upon ξ_1 or ξ_2, Eq. (B5) applied to Eq. (B1) yields

$$dA = \frac{9}{4(R+2)}\left(\frac{dy_{\max}}{1-y_{\max}} - \frac{dy_{\min}}{1-y_{\min}}\right). \tag{B6}$$

Using Eq. (B3) and (B4) to write

$$dy_{\min} = -(R+1)d\xi_1 + d\xi_2 \tag{B7}$$

and

$$dy_{\max} = d\xi_1 + d\xi_2 \tag{B8}$$

obtains

$$\frac{d\xi_1}{d\xi_2} = -\frac{E-1}{E+R+1} \, , \tag{B9}$$

where

$$E = \frac{1 - y_{\min}}{1 - y_{\max}} \, . \tag{B10}$$

If we introduce a phenomenologial form $L(y)$ for a Lorentz-invariant cutoff at the Landau singularity, and select Λ such that

$$y\big|_{K^2 = \Lambda^2} \equiv y_L = 1 \, . \tag{B11}$$

Equation (B1) becomes

$$A' = \lim_{\eta\to 0}\frac{9}{4(R+2)}\left(\int_{y_{\min}}^{y_L - \eta}\frac{L\,dy}{1-y} + \int_{y_L + \eta}^{\infty}\frac{L\,dy}{1-y}\right), \tag{B12}$$

where the prime denotes that Eq. (B1) is extended by the use of L in this formulation. As discussed in I, the principal-value prescription has been used with the infinitesimal η going to zero (symmetrically) at the Landau singularity. [As with Eq. (B1), the self-consistency condition requires that $A' = $ constant.]

Equation (B12) can further be refined by also including the fermion-mass-damping effect [active when $K^2 < m_i^2$; see Eq. (A4) and related discussion]. With this refinement Eq. (B12) becomes

$$A' = \frac{9}{8}\int_{y_{\min}}^{y_0}\frac{dy_1}{1-y_1}$$
$$+ \lim_{\eta\to 0}\frac{9}{4(R+2)}\left(\int_{y_0}^{y_L - \eta}\frac{L\,dy}{1-y} + \int_{y_L + \eta}^{\infty}\frac{L\,dy}{1-y}\right) , \tag{B13}$$

where

$$y_1 = \frac{\alpha}{3\pi}\ln\frac{K^2}{m_1^2} + \frac{\alpha}{3\pi}\ln\frac{K^2}{m_2^2} \, , \tag{B14}$$

$$y_0 = \xi_1 + \xi_2 - 2\xi_3 \, , \tag{B15}$$

and

$$y_{\min} = \xi_2 - \xi_1 \, . \tag{B16}$$

Proceeding as before, we obtain

$$dA' = \frac{9}{8}\left(\frac{dy_0}{1-y_0} - \frac{dy_{\min}}{1-y_{\min}}\right) + \lim_{\eta\to 0}\frac{9}{4(R+2)}\left[\frac{L(y_L - \eta)d(y_L - \eta)}{\eta} - \frac{dy_0}{1-y_0} - \frac{L(y_L + \eta)d(y_L + \eta)}{-\eta}\right] = 0 \, . \tag{B17}$$

Using Eqs. (B2) and (B11),

$$d(y_L - \eta) = d(y_L + \eta) = d\xi_1 + d\xi_2 \, , \tag{B18}$$

where the quantity η contributes no functional dependence. From Eq. (B16),

$$dy_{\min} = -d\xi_1 + d\xi_2 \tag{B19}$$

to replace Eq. (B7), and from Eq. (B15)

$$dy_0 = d\xi_1 + d\xi_2 \, . \tag{B20}$$

Using Eqs. (B18)–(B20) in Eq. (B17), and setting $dA' = 0$ yields

$$0 = \frac{d\xi_1 + d\xi_2}{2(1 - y_0)} - \frac{d\xi_2 - d\xi_1}{2(1 - y_{\min})}$$

$$+ \lim_{\eta \to 0} \frac{2L}{\eta} \frac{d\xi_1 + d\xi_2}{R + 2} - \frac{d\xi_1 + d\xi_2}{(1 - y_0)(R + 2)} , \tag{B21}$$

which reduces to

$$\frac{d\xi_1}{d\xi_2} = -\lim_{\eta \to 0} \frac{\dfrac{2L}{\eta} + \dfrac{R}{2(1 - y_0)} - \dfrac{R + 2}{2(1 - y_{\min})}}{\dfrac{2L}{\eta} + \dfrac{R}{2(1 - y_0)} + \dfrac{R + 2}{2(1 - y_{\min})}} \tag{B22}$$

as the formula for the slope $dF/d\xi$.

In the limit, Eq. (B22) may be written

$$\frac{d\xi_1}{d\xi_2} = -1 + \frac{R + 2}{E'} , \tag{B23}$$

where

$$E' \equiv \lim_{\eta \to 0} \frac{2L(1)(1 - y_{\min})}{\eta} . \tag{B24}$$

One can see that for $E' \gg 1$ Eq. (B23) is essentially equivalent to Eq. (B9).

Equation (B24) shows that E' will be a divergent quantity going as $\lim_{\eta \to 0} \eta^{-1}$ provided $y_{\min} < 1$. From the definition of $y_{\min}$ [Eq. (B16)], Eq. (5), and the self-consistent value of ξ found in I, one anticipates that $y_{\min} < 1$ will be satisfied in the physical region of the mirror plot ($\xi_1, \xi_2 > 0$). Therefore, while in this approximation E' is a divergent quantity, the slope is convergent to

$$\frac{d\xi_1}{d\xi_2} = -1 \tag{B25}$$

in the physical region of the mirror plot.

It is clear that Eq. (B25) obtains independently of the values A' and R, and furthermore that it does not depend upon the details of L as long as L is a continuous function at the Landau singularity, which one would expect from physical considerations. Consequently, even when one includes the (nonlinear) fermion-mass-damping effect, $\xi_1 = F(\xi_2)$ still is a straight line, degenerate with $\xi_2 = F(\xi_1)$ everywhere; the divergence of the photon propagator at the Landau singularity dominates the calculation.

It is useful to note that at the symmetry point $\xi_1 = \xi_2$ which, using Eq. (B16), gives $y_{\min} = 0$. Thus, at the symmetry point Eq. (B24) becomes

$$E' = \lim_{\eta \to 0} \frac{2L(1)}{\eta} . \tag{B26}$$

If, as discussed in Sec. VI C 3, one takes the Pauli exclusion principle into account, then the limiting value for η can be related to the number of (available) states N in the phase space associated with normalization volume V used for the calculation. As long as V is finite, then η is also

finite. From the discussion in Sec. VI C 3, for the one-photon approximation it is appropriate to set

$$\eta = f[(R + 2)N]^{-1} , \tag{B27}$$

where the (unknown) factor f is expected to be on the order of unity; f is to account for the uncertainty in the coefficient associated with the onset of the second Pauli effect.[35] In this case, Eq. (B23) becomes

$$\frac{d\xi_1}{d\xi_2} = -1 + \frac{1}{2L(1)Nf} . \tag{B28}$$

Thus at the symmetry point $1/[2L(1)Nf]$ is the one-photon estimate for ϵ_2.

APPENDIX C: N DEPENDENCE OF THE SELF-MASS SOLUTIONS

It is the purpose of this appendix to show that the locations of the self-mass solutions are independent of the effective number of phase-space states N, where N is introduced in Sec. V. The analysis to show this starts with the approximation that includes the phenomenological Lorentz-invariant cutoff at the Landau singularity and the (nonlinear) fermion-mass-damping effect. In this approximation, as shown in Appendix B, $d\xi_1/d\xi_2 = -1$ everywhere; $\xi_1 = F(\xi_2)$ is a straight line perpendicular to the symmetry axis on the mirror plot, $\xi_2 = F(\xi_1)$ being degenerate with $\xi_1 = F(\xi_2)$.

It was remarked in Sec. V that if the $(\xi_1 + \xi_2)$ symmetry of F is broken, the lines $\xi_1 = F(\xi_2)$ and $\xi_2 = F(\xi_1)$ will separate slightly. The intersection points of these curves then specify the location of the self-consistent solutions to the coupled self-mass equations, both symmetric and asymmetric, as depicted in Fig. 4.

An indicator of the separation of these two curves is the quantity

$$D(\xi_2) \equiv F(\xi_2) - F(F(\xi_2)). \tag{C1}$$

Line segments representing the quantity D are shown in Fig. 4. It is evident that the zeros of the function $D(\xi_2)$ give the locations of the self-consistent solutions to the problem. We note here that by the criterion of Eq. (9), those solutions with $dD/d\xi_2 > 0$ are stable, while those with $dD/d\xi_2 < 0$ are unstable.

Because of the symmetry between ξ_1 and ξ_2, a more convenient coordinate system in which to analyze this problem is one rotated by 45° from (ξ_1, ξ_2). That is, let

$$\zeta_1 = \frac{1}{\sqrt{2}}(\xi_1 + \xi_2), \quad \zeta_2 = \frac{1}{\sqrt{2}}(-\xi_1 + \xi_2). \tag{C2}$$

In terms of these new variables, it is useful

to define the function

$$\Delta(\zeta_2) = D(\xi_2) , \tag{C3}$$

where to be unambiguous, we define the argument ζ_2 of $\Delta(\zeta_2)$ as that specified by the argument ξ_2 on the line $\xi_1 = F(\xi_2)$ as indicated by the dots in Fig. 4. That is, $\zeta_2 = [\xi_2 - F(\xi_2)]/\sqrt{2}$.

For the initial (degenerate) approximation mentioned above, we see that $\Delta(\zeta_2) = 0$ for all ζ_2. Inclusion of the $(\xi_1 + \xi_2)$-symmetry-breaking effects leads to $\Delta(\zeta_2) \neq 0$ in general, but as required by permutation symmetry, leaves $\Delta(0) = 0$, the symmetric solution.

We now make the power-series expansion

$$\Delta(\zeta_2) = \sum_{n=1}^{\infty} a_n \zeta_2{}^n . \tag{C4}$$

By symmetry $a_0 = 0$, and has already been omitted from Eq. (C4). Now $\Delta(\zeta_2)$ is known to be small and goes to zero when $1/N$ goes to zero. Therefore, we assume that we can expand the coefficients a_n in the small parameter $N^{-1} \ll 1$. That is, we may set

$$a_n = \sum_{i=0}^{\infty} b_{in}\left(\frac{1}{N}\right)^i , \tag{C5}$$

where the b_{in} are independent of N. This step yields

$$\Delta(\zeta_2) = \sum_{n=1}^{\infty} \sum_{i=0}^{\infty} b_{in}\left(\frac{1}{N}\right)^i \zeta_2{}^n . \tag{C6}$$

When $N = \infty$, $\Delta(\zeta_2) = 0$, and Eq. (C6) reduces to

$$0 = \sum_{n=1}^{\infty} b_{0n} \zeta_2{}^n = 0 . \tag{C7}$$

Since Eq. (C7) is true for all ζ_2, it follows that

$$b_{0n} = 0 \tag{C8}$$

for all $n > 0$. Thus we can drop the $i = 0$ terms from Eq. (C6). For large N, we need only the leading, or $i = 1$, terms in Eq. (C6) and write

$$\Delta(\zeta_2) = \sum_{n=1}^{\infty} b_{1n} \frac{1}{N} \zeta_2{}^n \tag{C9}$$

as the appropriate equation for large N. When one solves Eq. (C9) for the roots of Δ, one obtains

$$\sum_{n=1}^{\infty} b_{1n} \zeta_2{}^n = 0 , \tag{C10}$$

an equation in ζ_2, independent of N.

One may now let the normalization volume for the problem become as large as one wants. As a consequence, N gets larger, and the curves $\xi_1 = F(\xi_2)$ and $\xi_2 = F(\xi_1)$ lie closer together causing $\Delta(\zeta_2)$ to approach zero. However, because Eq. (C10) is independent of N, the solution points of the coupled equation given by the roots of Δ, remain invariant as this limit is taken. Thus, in the limit of $N \to \infty$ we have $d\xi_1/d\xi_2 \to -1$, but still have discrete solutions with the possibility of asymmetric solutions.

[1] D. Fryberger, Phys. Rev. D **20**, 952 (1979).

[2] W. Heisenberg, in *1958 Annual Conference on High Energy Physics at CERN*, edited by B. Ferretti (CERN Scientific Information Service, Geneva, 1958); H. P. Dürr, W. Heisenberg, H. Mitter, S. Schleider, and R. Yamayaki, Z. Naturforsch. **14a**, 441 (1959); **16a**, 726 (1961).

[3] Y. Nambu, in *Proceedings of the Tenth Annual International Rochester Conference on High Energy Physics*, edited by E. C. G. Sudarshan, J. H. Tintot, and A. C. Melissinos (Interscience, New York, 1960); G. Jona-Lasinio and Y. Nambu, Phys. Rev. **122**, 345 (1961); **124**, 246 (1961); J. Goldstone, Nuovo Cimento **19**, 154 (1961).

[4] M. Baker and K. Johnson, Phys. Rev. D **3**, 2516 (1971). This paper contains references to their earlier work.

[5] K. Johnson, Phys. Lett. **5**, 253 (1963); M. Baker, K. Johnson, and B. W. Lee, Phys. Rev. **133**, B209 (1964).

[6] J. Goldstone, Nuovo Cimento **19**, 154 (1961); J. Goldstone, A. Salam, and S. Weinberg, Phys. Rev. **127**, 965 (1962).

[7] J. D. Bjorken and S. D. Drell, *Relativistic Quantum Fields* (McGraw-Hill, New York, 1965), p. 290.

[8] L. D. Landau, in *Niels Bohr and the Development of Physics*, edited by W. Pauli (Pergamon, London, 1955), p. 52; L. D. Landau and I. Pomeronchuk, Dok. Akad. Nauk SSSR **102**, 489 (1955); L. D. Landau, A. A. Abrikosov, and I. Halatnikov, Nuovo Cimento Suppl. **3**, 80 (1959). The last contains references to earlier works. Translations of the Russian articles may be found in *Collected Papers of L. D. Landau*, edited by D. ter Haar (Pergamon, Oxford, 1965).

[9] There is by now extensive use of the Borel summation technique to study high-order behavior of perturbation series in quantum field theory. See, e.g., L. N. Lipatov, in *Proceedings of the Eighteenth International Conference on High Energy Physics, Tbilisi, 1976*, edited by N. N. Bogoliubov *et al.* (JINR, Dubna, U. S. S. R., 1977); Zh. Eksp. Teor. Fiz. **72**, 411 (1977) [Sov. Phys.–JETP **45**, 216 (1977)]; Pis'ma Zh. Eksp. Teor. Fiz. **24**, 179 (1976) [JETP Lett. **24**, 157 (1976)]; E. Brézin, J. C. LeGuillou, and J. Zinn-Justin, Phys. Rev. D **15**, 1558 (1977); G. Parisi, Phys. Lett. **66B**, 167 (1977); D. V. Shirkov, Lett. Nuovo Cimento **18**, 452 (1977); C. Itzykson, G. Parisi, and J.-B. Zuber, Phys. Rev. Lett. **38**, 306 (1977); Phys. Rev. D **16**, 996 (1977); R. Balian, C. Itzykson, G. Parisi, and J. B. Zuber, *ibid.* **17**, 1041 (1978).

[10] B. Lautrup, Phys. Lett. **69B**, 109 (1977).

[11] A more complete discussion of this point is given in I. In addition to Ref. 8, it is also of interest to read

C. R. Hagen and M. A. Samuel, Phys. Rev. Lett. 20, 1405 (1968) and references therein.

[12]J.-E. Augustin et al., Phys. Rev. Lett. 34, 233 (1975); B. L. Beron et al., ibid. 33, 663 (1974); H. Newman et al., ibid. 32, 483 (1974); E. Hilger et al., Phys. Rev. D 15, 1809 (1977). A nice discussion of an indirect limit to the pointlike structure of the electron and muon determined by a comparison of theoretical and experimental magnetic anomalous moments has been given by S. J. Brodsky and S. D. Drell, Phys. Rev. D 22, 2236 (1980), but this limit of $\sim 10^{-21}$ cm still falls well short of the Planck length of $\sim 10^{-33}$ cm.

[13]It was originally suggested by Landau and his collaborators, Ref. 8, that the gravitational interaction may play some role in short-distance QED. That gravitation might furnish a cutoff for QED has also been investigated by others: B. S. DeWitt, Phys. Rev. Lett. 13, 114 (1964); I. B. Khriplovich, Yad. Fiz. 3, 375 (1966) [Sov. J. Nucl. Phys. 3, 415 (1966)]; A. Salam and J. Strathdee, Lett. Nuovo Cimento 4, 101 (1970); C. J. Isham, A. Salam, and J. Strathdee, Phys. Rev. D 3, 1805 (1971); Phys. Lett. 35B, 585 (1971); Phys. Rev. D 5, 2548 (1972); G. Rosen, ibid. 4, 275 (1971); H. Fanchiotti, C. A. Garcia Canal, H. Girotti, and H. Vucetich, Nucl. Phys. B34, 307 (1971); Lett. Nuovo Cimento 2, 1001 (1971); M. A. Markov, Zh. Eksp. Teor. Fiz. 64, 1105 (1973) [Sov. Phys.–JETP 37, 561 (1973)].

[14]E. T. Whittaker and G. N. Watson, A Course in Modern Analysis, fourth edition (Cambridge University Press, Cambridge, England, 1927), p. 154.

[15]In an analysis along different lines, P. I. Fomin, Fiz. Elem. Chastits At. Yadra 7, 687 (1976) [Sov. J. Part. Nucl. 7, 269 (1976)], has obtained an explicit relationship (numerically similar, not identical to that in I) between M_P and the QED ultraviolet cutoff.

[16]Typical results and references to other data are found in J.-E. Augustin et al., Phys. Rev. Lett. 34, 764 (1975). Recent high-energy results have been discussed by B. H. Wiik, in High Energy Physics—1980, proceedings of the XXth International Conference, Madison, Wisconsin, edited by L. Durand and L. G. Pondrom (AIP, New York, 1981).

[17]M. Baker and S. L. Glashow, Phys. Rev. 128, 2462 (1962).

[18]G. Feinberg, P. Kabir, and S. Weinberg, Phys. Rev. Lett. 3, 527 (1959); N. Cabibbo and R. Gatto, ibid. 5, 114 (1960).

[19]These eigenvalues, ±1, as constants of the motion will lead to a multiplicative conservation law for muons and electrons. It should be remarked, however, that there might be other conservation laws active which could obscure this multiplicative relationship. The question of whether muons and electrons are governed by multiplicative or additive quantum numbers was raised some time ago by G. Feinberg and S. Weinberg, Phys. Rev. Lett. 6, 381 (9161); Phys. Rev. 123, 1439 (1961).

[20]J. D. Boman et al., Phys. Rev. Lett. 42, 556 (1979); S. Parker et al., Phys. Rev. 133, B768 (1964); P. Depommier et al., Phys. Rev. Lett. 39, 1113 (1977); H. P. Povel et al., Phys. Lett. 72B, 183 (1977); A. vander Schaaf et al., Nucl. Phys. A340, 249 (1980).

[21]Q. Bui-Duy, Prog. Theor. Phys. 45, 605 (1971).

[22]Goldstone, Ref. 6, also noted that no such bosons would be generated by the breaking of a discrete symmetry.

[23]While detailed calculations of the energy of the vacuums will not be pursued in this paper, it is relevant to remark that due to the curvature of $F(\xi)$, see Fig. 4(c), the inequalities between the symmetric mass solutions and the asymmetric mass solutions in this model are the same as those given by the line segments (OA) and (OI) in the vacuum energy difference equation just prior to Eq. (5) of Ref. 21. Consequently, this self-consistency stability criterion as applied to this model gives a result in agreement with that found by Bui-Duy's direct calculation of the two vacuum states (Ref. 21).

[24]The term "hadronic" as it is used here also includes a heavy leptonic part. Since it is assumed that these heavy leptons are not subject to a permutation-invariant relationship with the muon or electron, they will play no special role in the μ-e mass splitting. (It would also be possible to extend the notions of permutation symmetry to include these heavy leptons.)

[25]J. C. Ward, Phys. Rev. 78, 182(L) (1950).

[26]Higher-order graphs which also contribute nonlinearities were also investigated. The graphs go one step beyond the vacuum polarization denominator of Eq. (A11I) including corrections to the vacuum polarization loops. See Ref. 7, Eq. (19.161), p. 372, for appropriate formulas. The curvature due to these graphs was found to be several orders of magnitude smaller than that due to the fermion-mass-damping effect, and hence has been neglected.

[27]V. F. Weisskopf, Phys. Rev. 56, 72 (1939).

[28]W. Heitler, The Quantum Theory of Radiation, third edition (Oxford University Press, London, 1954), p. 294.

[29]J. D. Bjorken and S. D. Drell, Relativistic Quantum Mechanics (McGraw-Hill, New York, 1964), p. 165.

[30]R. P. Feynman, Phys. Rev. 76, 749 (1949).

[31]Reference 7, p. 189.

[32]For the symmetric solutions, which were investigated in I, the influence of the first Pauli effect is negligible because as a practical matter, these Pauli-excluded pieces make an infinitesimal contribution to the final result; the number of Pauli-excluded states is an infinitesimal fraction of the total number of available intermediate states. (A similar remark prevails for calculations like that of Lautrup.[10])

[33]E. Schrödinger, Sitzber. Preuss. Akad. Wiss. Physik-Math. 24, 418 (1930).

[34]We rely on the (presumed) convergence of the summation used in this model and the random nature of the Pauli-excluded states to assert that the vanishingly small fraction of Pauli-allowed pieces do not sum to a significant contribution in the final result. This argument finds support in the studies of C. M. Bender and T. T. Wu, Phys. Rev. Lett. 37, 117 (1976) who show that (except for non-Borel-summable graphs, e.g., the Landau singularity) statistical considerations dominate the high-order behavior of the perturbation series.

[35]There is an intrinsic uncertainty in this factor because R is an effective number of constituents and not a physical count. However, overlooking this question, Eq. (B27) indicates that the factor $R+2$ cancels out.

[36]D. Fryberger, in preparation. Other models proposing

composite fermion structure include T. Massam and
A. Zichichi, Nuovo Cimento 43A, 227 (1966); H. J.
Lipkin, Riv. Nuovo Cimento 1, 134 (1969); Phys. Rep.
8C, 172 (1973); O. W. Greenberg and C. A. Nelson,
Phys. Rev. D 10, 2567 (1974); G. R. Kalbfleisch and
E. C. Fowler, Nuovo Cimento 19A, 173 (1974); J. C.
Pati and Abdus Salam, Phys. Rev. D 10, 275 (1974);
K. Matumoto, Prog. Theor. Phys. 52, 1973 (1974);
J. C. Pati, A. Salam, and J. Strathdee, Phys. Lett.
59B, 265 (1975); O. W. Greenberg, Phys. Rev. Lett.
35, 1120 (1975); E. Novak, J. Sucher, and C. H. Woo,
Phys. Rev. D 16, 2874 (1977); H. Terazawa, *ibid.* 22,
184 (1980); G. Shaw, Phys. Lett. 81B, 343 (1979);
H. Harari, *ibid.* 86B, 83 (1979); M. A. Shupe, *ibid.*
86B, 87 (1979); J. G. Taylor, *ibid.* 88B, 291 (1979);
D. Fryberger, Lett. Nuovo Cimento 28, 313 (1980);
H. Chao-Shang and D. Yuan-Ben, Institute of Theore-
tical Physics, Academia Sinica Report No. AS-ITiP-
80-015, 1980 (unpublished).

[37]It is not unreasonable to suppose that a form of "in-
finite-momentum" QED applicable to distances less
than the Landau length can be developed. Because
of the conformal invariance of electromagnetism and
the massless Dirac equations, we would expect the
"self-mass" of this QED to be expandable in a per-
turbation series of Feynman graphs which would be
isomorphic to those of Σ in the usual QED. In fact,
implicit in the assumption of analytic continuability
is the existence of this infinite-momentum series.
Thus, the logic that leads to a Landau singularity in
the usual QED would also lead to a Landau singularity
in this QED, and they would (presumably) join at M_L.
In this case, expecting Pauli saturation in both QED's
would lead to the expectation of symmetric modifi-
cations at M_L of the analytically continued photon
propagator.

[38]While one anticipates a large sensitivity to numerical
error in the self-consistent determination of Λ from
the observed fermion masses (a sum of the parameters
ξ_i must be exponentiated), setting $\Lambda = M_P$ merely
furnishes a scale for the problem, the arbitrariness
of which will cancel to first order in the ratio m_μ/m_e.

[39]The error here does not appear to be large. A one-

gluon correction to a quark vacuum polarization loop
yields $\sim 20\%$ increase over the QED vacuum polariza-
tion loop alone: J. Ellis, in *Proceedings of the 9th
International Symposium on Lepton and Photon Inter-
actions at High Energy,* edited by T. B. W. Kirk and
H. D. I. Abarbanel (Fermilab, Batavia, Ill., 1980),
p. 412.

[40]Such an extrapolation, in a somewhat different context,
has been suggested by V. G. Kadyshevskii, Fiz. Elem.
Chastits At. Yadra, 11, 5 (1980) [Sov. J. Part. Nucl.
11, 1 (1980)].

[41]Since the errors on the mass splitting are so large,
one cannot determine from the calculations here
whether the initial permutation symmetry is between
e and μ or e and τ. In the latter case, anticipating
the same cancellations in the mass ratios, we would
write $m_\tau/m_e = m_T/m_\mu$ instead of Eq. (20), giving the
same prediction: $m_T \sim 380$ GeV/c^2. However, it is
clear that for more detailed calculations, the predicted
m_T would differ in these two cases.

[42]K. Tennakone and S. Pakvasa, Phys. Rev. D 6, 2494
(1972). This model was published before the discovery
of the τ, which it did not predict. Thus for the physics
of their model to be correct, the τ would have to be
the lightest lepton of another sequence of leptons.

[43]G. Rosen, Int. J. Theor. Phys. 17, 1 (1978).

[44]S. Blaha, Lett. Nuovo Cimento 22, 425 (1978).

[45]J. D. Bjorken, Report No. SLAC-PUB-2195, 1978
(unpublished).

[46]A. Pais, in *High Energy Physics in the Einstein
Centennial Year,* proceedings of the Orbis Scientiae,
Coral Gables, 1979, edited by A. Perlmutter,
F. Krause, and L. F. Scott (Plenum, New York, 1979),
p. 79.

[47]A. O. Barut, Phys. Rev. Lett. 42, 1251 (1979); 43,
1057 (E) (1979).

[48]W. Krolikowski, Acta Phys. Pol. B 10, 767 (1979).

[49]P. Caldirola, Lett. Nuovo Cimento 27, 225 (1980).

[50]Reference 7 or Ref. 29.

[51]G. C. Wick, Phys. Rev. 96, 1124 (1954).

[52]Reference 29, Eq. (8.22).

[53]B. O. Pierce, *A Short Table of Integrals,* third edition
(Ginn, Boston, 1929), formula 857.